

In Situ, Time-Resolved Normal Incidence Reflectance Spectroscopy of Polycrystalline Platinum Microelectrodes in Aqueous Electrolytes

Iosif Fromondi, Ping Shi, Atsushi Mineshige, and Daniel A. Scherson*

Department of Chemistry, Case Western Reserve University, Cleveland, Ohio 44106-7078

Received: November 18, 2004

In situ normal incidence reflectance spectra of polycrystalline Pt microelectrodes have been monitored as a function of the applied potential in aqueous 0.5 M H₂SO₄ using a He–Ne laser source (633 nm) and a beam splitter/microscope objective arrangement. Data recorded during voltammetric cycles in Ar-purged solutions revealed a linear correlation between the normalized change in reflectance, $\Delta R/R = (R_s - R_{\text{ref}})/R_{\text{ref}}$ (where R_s and R_{ref} are the light intensities measured by the detector at the sampling, s , and reference potentials, ref , respectively), and the extent of oxidation of the Pt surface over a wide coverage range. Reflectance spectra were also collected in CO-saturated 0.5 M H₂SO₄ during chronocoulometric measurements involving judiciously selected limits for both the potential step and duty cycle parameters. Analysis of these results made it possible to extract contributions to the current derived from oxide formation during oxidation of adsorbed and bulk CO, based strictly on the optical response.

Introduction

The coupling of microelectrodes and optical techniques has opened new prospects for the study of interfacial processes in the submicrosecond domain. This strategy is being implemented in our laboratory for monitoring the dynamics of adsorbed species on electrode surfaces. Preliminary efforts have focused on the combined use of second harmonic generation and single-crystal microfaceted spherical single crystals for determining the rates of the $\text{c}(2 \times 2)\text{-3CO} \rightarrow \sqrt{19} \times \sqrt{19} \text{R23.4}^\circ\text{-13CO}$ phase transition on Pt(111), as well as the rates of oxidation of adsorbed CO on the same low index face.¹ Although such facets display a very low density of defect sites, it has not been possible so far to produce faceted microspheres of sufficiently small diameter to decrease the time constant of the cell well below the microsecond range. Furthermore, since the spheres are immersed in the electrolyte, no direct correlations could be drawn between the optical (local) and electrical (global) responses.

The present contribution describes a novel experimental arrangement that allows reflectance spectroscopy measurements to be performed at normal incidence on Pt(poly) microelectrodes of a diameter as small as 11.5 μm . The results obtained have not only been found to be in excellent agreement with those reported earlier for larger electrodes, but a judicious choice of duty cycle parameters has made it possible to monitor Pt oxide formation Pt(poly) during oxidation of adsorbed and bulk CO in CO-saturated 0.5 M H₂SO₄ solutions relying exclusively on the optical response.

Experimental Section

Reflectance measurements were performed using a medium power (ca. 15–17 mW) HeNe laser (JAS Uniphase model

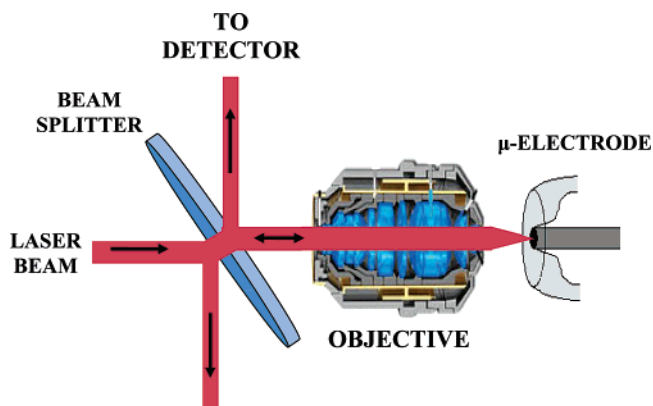


Figure 1. Schematic diagram of the set up employed for normal incidence reflectance spectroscopy measurements on microelectrodes. Dimensions are not to scale for clarity.

1144P, 633 nm) as the light source, aimed through a set of high reflectance mirrors (Newport) at the surface of a beam splitter (CVI Laser Corporation, $R_s/T_s = 50/50$, 45°, 630 nm) at an angle of incidence of 45°. As shown in Figure 1, the transmitted beam was then focused onto the surface of a polycrystalline Pt working microelectrode at normal incidence using a microscope objective (Olympus 20 \times /0.40). Upon reflection from the electrode, the beam passed through the objective, impinging on the splitter from the opposite side, and was then focused using a borosilicate lens onto a battery-biased Si PIN detector (Newport, model 818-BB-20) connected to a battery-operated current preamplifier (Hamamatsu C6438-01). The output signal of the latter device was then fed, to the input of a 0.5 GHz oscilloscope (Tektronix TDS 744A) for monitoring and further processing.

Microelectrodes were made by sealing a 25 (or 11.5) μm Pt wire (99.95% Alfa Aesar) into a glass capillary to yield, after polishing, a disk-shaped Pt surface. Particular care was exercised

* To whom correspondence should be addressed.

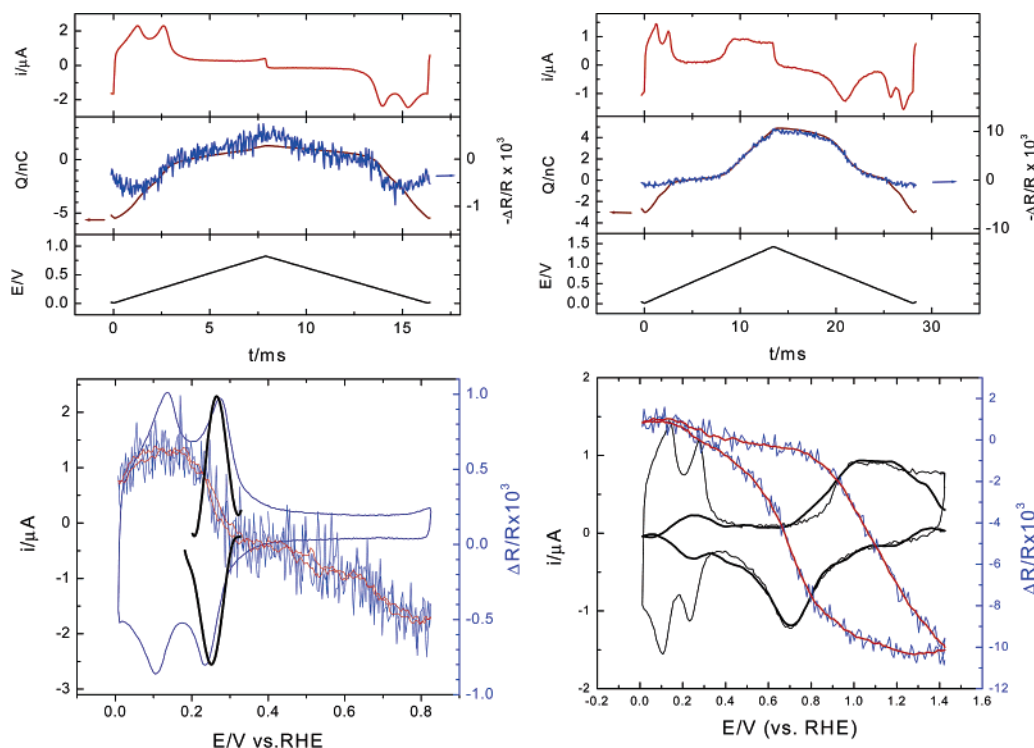


Figure 2. Upper panels: Time dependence of the current (top) and potential (bottom subpanel) for a 25 mm (diameter) Pt microdisk electrode in deaerated 0.5 M H_2SO_4 in the regions $0.0 < E < 0.84$ V (Left Panel) and $0.0 < E < 1.45$ V (Right Panel) at a scan rate $\nu = 100$ V/s. The smooth curves in the center subpanels are the charges obtained by integrating the current whereas the jagged curves are the changes in reflectance with time recorded simultaneously. Lower panels: Cyclic voltammograms (smooth thin curves, left axes) and $\Delta R/R$ ($R_{\text{ref}} = 0.4$ V, jagged curve, right axes) vs E constructed based on the data shown in these figures are 10 -pt adjacent average (10 pt. AA). Also shown in thicker lines in these figures are $1/R(\partial R/\partial E)$ vs E curves obtained from the fitted optical data (left panel) and the 7 pt. AA smoothed curve of derivative of the smoothed optical data (right panel) in the potential regions in question, for which the amplitudes and signs were adjusted so as to match the current in the voltammogram (see text for other details).

to decrease the area of contact between the wire and the surrounding glass casing in order to minimize effects due to stray capacitances. All glassware, Teflon pieces, and electrodes were thoroughly cleaned by first soaking in concentrated $\text{H}_2\text{SO}_4/\text{H}_2\text{O}_2$ (90/10 by volume) overnight and then boiling several times in ultrapure water.

All experiments were performed at room temperature in Ar-purged (Praxair 5.0) or CO-saturated (Matheson Tri-Gas) ultrapure aqueous 0.5 M H_2SO_4 (H_2SO_4 , Ultrex, 18.3 M Ω water, Barnstead water purifier) in a three-electrode system, using a reversible hydrogen electrode in the same solution (RHE) as a reference. The RHE was prepared by generating electrochemically a hydrogen bubble at the top of a capillary filled with 0.5 M H_2SO_4 incorporating a Pt wire in contact with both the H_2 gas bubble and the electrolyte. To avoid contamination with CO, the RHE was placed in a separate compartment connected to the main body of the cell (a 1 cm path length quartz cuvette) via a Teflon tubing.

Results and Discussion

Shown in smooth lines in the left upper panel, Figure 2, are the averaged current (i , top, total number of acquisitions, $N = 7900$), integrated charge (Q , assuming $Q = 0$ for $E = 0.4$ V, middle) and potential (E , bottom) curves as a function of time, over the range $0 < E < 0.84$ V recorded for a 25 mm (diameter) polycrystalline Pt microdisk electrode in deaerated 0.5 M H_2SO_4 at a scan rate of 100 V/s. Similar data collected over the range $0 < E < 1.45$ V vs RHE for $N = 1764$, are given in the right upper panel in this figure. Also plotted in the middle sub-panel of both upper panels are average $-\Delta R/R$ ($\lambda = 633$ nm, $R_{\text{ref}} = 0.4$ V, see jagged curve) vs t recorded simultaneously involving

$N = 33376$ and 4766 acquisitions for the shorter and longer E ranges, respectively, where the amplitudes of the optical signals were arbitrarily adjusted to match that of the charges Q . The i vs E (thin line, left ordinate) and $\Delta R/R$ vs E data (jagged curve, right ordinate) are displayed in cyclic form in the corresponding lower panels in this figure. The continuous line through the optical data represent the 10-point adjacent average (10 pt. AA) and compares very well with those reported much earlier for larger Pt electrodes by Bewick et al. in 1 M H_2SO_4 over a rather wide range of wavelengths and angles of incidence, for both p and s polarization.²

As evident from these results, the dependence of $\Delta R/R$ on the applied potential in the double layer region, i.e., $0.3 < E < 0.8$ V, is almost linear (see left lower panel, Figure 2). Also shown in this panel is a plot of $1/R(\partial R/\partial E)$ vs E in the range $0.2 < E < 0.3$ V obtained after fitting the reflectance data with an arbitrary function (see solid thick line), where, for purely display purposes, the sign (and magnitude) of $1/R(\partial R/\partial E)$ was adjusted so as to match the corresponding voltammetric peak. As indicated, this optically derived curve tracks rather well the peak(s) in question. A close correlation between the optical and electrochemical response was found recently in our laboratory for the so-called butterfly peaks of Pt(111) in 0.1 M H_2SO_4 .³

The averaged voltammetric and $\Delta R/R$ vs E curves recorded simultaneously in the range $0 < E < 1.45$ V at 100 V/s (see smooth thin line and jagged line, respectively, in the lower right panel, Figure 2) were found to be in excellent agreement with those reported elsewhere for much larger Pt(poly) electrodes and substantially lower scan rates.^{4,5} Furthermore, plots of $-\Delta R/R$ vs t (jagged curve) and charge, Q (smooth curve) vs t obtained by direct integration of the voltammetric scans using

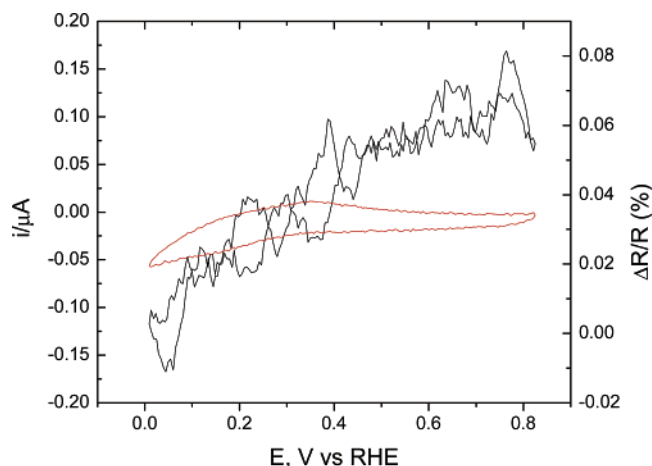


Figure 3. Cyclic voltammogram (smooth curve, left ordinate) and averaged (total number of acquisitions $N > 20\,000$, 10 pt. AA smoothing) $\Delta R/R$ ($R_{\text{ref}} = 0.1$ V, jagged curve, right ordinate) recorded simultaneously for a 25 mm (diameter) Pt microdisk electrode in CO-saturated 0.5 M H_2SO_4 in the potential range $0.0 < E < 0.8$ recorded at a scan rate $\nu = 5$ V/s.

$Q = 0$ nC at $E = 0.40$ V as the integration limit (see middle subpanel in the upper right panel, Figure 2), virtually overlapped the oxide formation and reduction regions, regardless of the direction of the scan. Since oxide formation and oxide reduction occur over a much different potential range, it may be concluded that the amount of oxide on the surface and not the potential determines the magnitude of the optical signal. This point is clearly illustrated by overlaying the $1/R(\partial R/\partial E)$ vs E curve directly on the voltammogram (see thick solid line in the lower

right panel, Figure 2), where the (arbitrary) ordinate was once again adjusted so as to match the voltammetric features. It is precisely this property that will allow the rates of oxide formation during oxidation of adsorbed and bulk CO oxidation to be determined based strictly on the optical response (see section below). As has been noted by other authors, $1/R(\partial R/\partial E)$ decreases as a function of the applied potential for $E > 1.2$ V,^{5,6} an effect that may be attributed to the formation of a different type of Pt oxide on the surface. For this reason, all measurements to be presented in the following section involved potentials $E < 1.2$ V.

Oxidation of Adsorbed and Bulk CO

In situ reflectance spectroscopy measurements in CO-saturated 0.5 M H_2SO_4 performed under otherwise identical conditions as those described in the previous section yielded in the region $0 < E < 0.8$ V (see Figure 3) a fairly linear behavior with a slope of precisely the opposite sign compared to that found in an Ar-purged solutions (see, for example, lower left panel in Figure 2). Although speculative, it is tantalizing to suggest that the factors responsible for this behavior have the same origin as those invoked to explain the linear change in the frequency of the CO stretching band (or Stark shift) observed in the in situ infrared reflection absorption spectra (IRAS) in the same potential region.⁷

A series of experiments were then performed in which the potential was stepped from a value negative enough for CO adsorption to ensue, E_{ads} , to a value sufficiently positive for adsorbed CO to undergo full oxidation, E_{ox} , but still within the region in which the optical signal is proportional to the extent

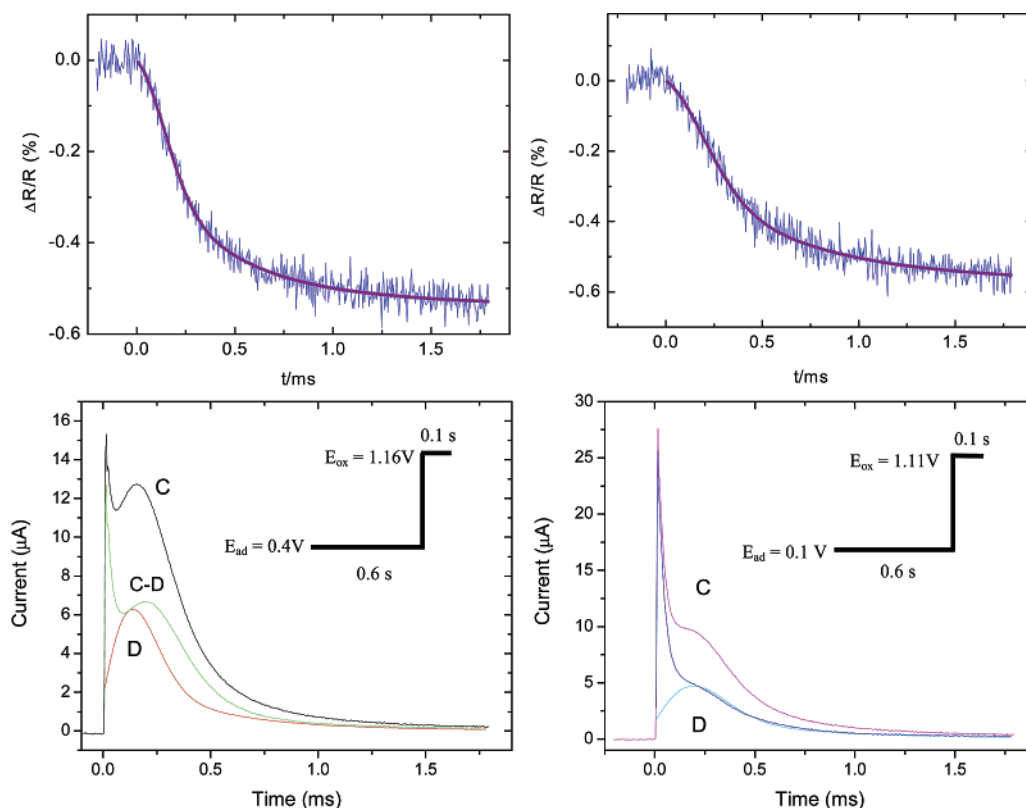


Figure 4. Upper panels: Normalized reflectance, $\Delta R/R$ ($R_{\text{ref}} = 0.4$ V (left panel); 0.1 V (right panel), jagged curve) for a 25 mm (diameter) Pt microdisk electrode in CO-saturated 0.5 M H_2SO_4 collected during a potential step from 0.4 to 1.16 V ($N = 10\,432$, left panel) and from 0.1 to 1.11 V ($N = 6148$, right panel) recorded simultaneously. The smooth curves are arbitrary pseudo-Voigt function fits. Lower panels: Derivatives of the fits to the optical data in the corresponding upper panels converted to a current (see curve D and text for details) and chronopotentiometric response (i vs t , curve C) recorded simultaneously. The curves labeled as C–D represent contributions to the current due to processes other than oxide formation (see text).

of oxidation, $E_{\text{ox}} < 1.2$ V. Since readsorption of CO on Pt is (at least partially) under diffusion control, the time allowed to form the adsorbed CO layer at E_{ads} was set at 0.6 s. Since under the conditions of this experiment the oxidation of adsorbed CO is kinetically controlled, the electrode was polarized at E_{ox} for only 0.1 s. Shown in the upper panels in Figure 4 are the results of two of such measurements involving values of $E_{\text{ads}} = 0.4$ V and $E_{\text{ox}} = 1.16$ V ($N = 10\,432$) and $E_{\text{ads}} = 0.1$ V and $E_{\text{ox}} = 1.11$ V ($N = 6148$), as specified explicitly in the inserts in the lower panels, where the jagged curves represent the actual averaged raw optical data and the smooth curves are arbitrary pseudo-Voigt function fits. The lower panels display the derivative of the fits to the data in the corresponding upper panels converted to a current, based on the one-to-one correlation found between the optical response and the charge associated with formation of the surface oxide (see curve D). These results make it possible to extract from the measured current (C, lower panels) contributions to the current due to processes other than oxide formation, which will include predominantly oxidation of adsorbed and solution phase CO (see curves C–D, lower panels). It is expected that systematic

studies of this type will unveil important aspects of CO oxidation not accessible with conventional electrochemical techniques.

In summary, the combination of normal incidence UV–visible reflectance spectroscopy and microelectrodes offers improved means of monitoring in situ dynamic aspects of electrode processes involving adsorbed species. Further refinements involving charge injection currently underway in our laboratories are expected to improve the time response of the system down to the submicrosecond regime.

References and Notes

- (1) Pozniak, B.; Scherson, D. A. *J. Am. Chem. Soc.* **2003**, *125*, 7488.
- (2) Bewick, A.; Tuxford, A. M. *J. Electroanal. Chem. Interfacial Electrochem.* **1973**, *47*, 255.
- (3) Fromondi, I.; Lopez Cudero, A.; Feliu, J.; Scherson, D. A. *J. Electrochem. Soc.* (in press).
- (4) Collas, N.; Beden, B.; Leger, J. M.; Lamy, C. *J. Electroanal. Chem.* **1985**, *186*, 287.
- (5) Nakabayashi, S.; Tamura, K.; Uosaki, K. *Bull. Chem. Soc. Jpn.* **1998**, *71*, 67.
- (6) Nakabayashi, S.; Yagi, I.; Sugiyama, N.; Tamura, K.; Uosaki, K. *Surf. Sci.* **1997**, *386*, 82.
- (7) Lambert, D. K. *Electrochim. Acta* **1996**, *41*, 623.